Morphology and orientational order of nematic liquid crystal droplets confined in a polymer matrix

Frédérick Roussel*
Laboratoire de Thermophysique de la Matière Condensée, Equipe de l'UPRESA CNRS 8024, Université du Littoral–Côte d'Opale, MREID, 59140 Dunkerque, France

Cécile Canlet† and Bing M. Fung
Department of Chemistry, University of Oklahoma, Norman, Oklahoma 73019
(Received 19 March 2001; published 9 January 2002)

The orientational order of nematic liquid crystal (LC) droplets confined in a polymer matrix is investigated by ^{13}C-NMR. Different morphologies exhibiting various cavity sizes were obtained by changing the LC fraction. The phase diagram has been established by polarized optical microscopy exhibiting a typical upper critical solution temperature shape. The nematic order increases with decreasing droplet size which may result from increased polymer/LC surface contacts in smaller cavities. The nematic fraction of 4-*n*-pentyl-4′-cyanobiphenyl (5CB) contained in the droplets was calculated by integrating the NMR peaks, then fitted using a simple theoretical model and compared with differential scanning calorimetry results. NMR investigations in the aliphatic region of the spectra have shown that the 2-ethyl hexyl fragment of the polymer chain is partially ordered at the polymer/LC interface due to interdigitation with 5CB molecules. Above the nematic-isotropic transition temperature, a weak pretransitional behavior is shown by the polymer.

DOI: 10.1103/PhysRevE.65.021701 PACS number(s): 61.30.−v, 64.70.Md, 64.75.+g, 42.70.Df

I. INTRODUCTION

Liquid crystals (LC) in complex geometries [1] have attracted considerable attention because of several interesting physical phenomena resulting from strong surface effects between the LC and the host [2]. Schwalb and Deeg [3] and Cramer *et al.* [4] showed that thermodynamic phases can be induced or suppressed by the confinement, and Golemme *et al.* [5] provided experimental demonstration confirming the Sheng's prediction [6,7] that the nematic-isotropic (N-I) coexistence curve terminates at a critical enclosure size. Indeed, for sufficiently small droplets the isotropic phase is replaced by a paranematic phase and the I-N transition is replaced by the continuous evolvment of order.

Studies of confined LC phases have been performed in numerous materials like porous filters (e.g., Anopore and Nucleopore membranes) [8,9], polymer matrices [e.g., polymer-dispersed liquid crystals (PDLC) and polymer-stabilized cholesteric textures (PSCT)] [1,10], and in various types of porous glasses, silica gels, and aerosils [11,12]. For the two first categories, the cavities are fairly well defined and ordered, whereas for glasses the pores are characterized by irregular sizes and shapes. PDLC and PSCT have found great interest because of their promising use in electro-optical devices, such as flexible displays and switchable windows [1,10]. Among the main aspects governing the electro-optical performances (i.e., transmission properties, drive voltage, switching times, etc.) of these materials are the morphology of the films, the concentration of LC, the surface anchoring conditions for the LC at the polymer interface, and the order parameter of the confined LC [10,13–17].

Order and dynamics of mesogenic molecules confined in porous materials or constrained by a polymer network have been widely studied by NMR [18], dielectric spectroscopy [4,19], birefringence measurements [20], and ac calorimetry [21]. Among these techniques, deuterium NMR and NMR relaxometry have proved to be useful tools to probe the effect of confinement on the molecular orientational ordering and the surface-induced order [4,5,18,22–30]. Although the application of ^{13}C-NMR to study bulk LC offers important information [18,31,32], this technique has been less used to investigate LC confined to micrometer-sized cavities. In 1991, Guo and Fung [33] reported a convenient ^{13}C-NMR method for the determination of order parameters of bulk LC from chemical shift anisotropy measurements. In this paper, this method is applied to determine the orientational ordering of LC [4-*n*-pentyl-4′-cyanobiphenyl (5CB)] droplets confined in a poly(ethylhexylacrylate) matrix.

Section II describes the preparation of the samples and explains how the experiments were carried out. In Sec. III A the phase behavior and the morphology of the PDLC samples are investigated by polarized optical microscopy (POM) and differential scanning calorimetry (DSC) measurements are described. ^{13}C-NMR experiments of PDLC samples prepared with various droplet sizes and LC order parameter calculations are described in Secs. III B 1, III B 2, and III B 3. The fractional amount of LC contained in the droplets is also estimated by NMR and compared with DSC results (Sec. III B 4). Section III B 5 deals with the surface induced order at the polymer/LC interface. Finally, in Sec. IV a summary of the conclusions is given.

*Author to whom correspondence should be addressed. Email address: Frederick.Roussel@purple.univ-littoral.fr

†Present address: Laboratoire des Xenobiotiques INRA, Boîte Postale 3, 31931 Toulouse Cedex 9, France.

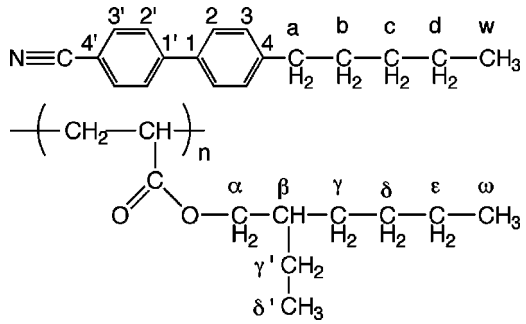

FIG. 1. Chemical structures of the liquid crystal 5CB (top, the aromatic protons are omitted for clarity) and of the polymer poly(2-ethylhexylacrylate) PEHA (bottom).

II. EXPERIMENT

The liquid crystal 4-*n*-pentyl-4′-cyanobiphenyl (5CB, Fig. 1, top) was used during this work because many thermodynamic and NMR data are available in the literature [1,10,31]. 5CB was purchased from Aldrich, Saint Quentin-Fallavier, France. It exhibits a nematic (*N*) phase between the crystalline (Cr) and isotropic (*I*) states in the temperature range 25.5–35.3 °C [34]. 5CB is easily supercooled from the *N* state to -10 °C.

The monofunctional acrylate monomer 2-ethylhexylacrylate (EHA) was used as precursor of the polymer because no aromatic carbons are present in the polymer backbone (Fig. 1, bottom). The possible overlappings of the NMR signals of polymer EHA (PEHA) and 5CB are then reduced, making it easier to measure the LC chemical shifts (see Sec. III B). Moreover, PEHA is fully isotropic in the temperature range of interest [35]. EHA was supplied from Aldrich (Saint Quentin Fallavier, France) and used without further purification. The UV polymerization was induced by 2 wt. % of Darocur 1173 (Ciba, Rueil Malmaison, France) with respect to the amount of monomer used.

The monomer and the liquid crystal were mixed together at room temperature for several hours. Samples for optical microscopy were prepared by placing one drop of the mixture between standard glass slides resulting in a film thickness of approximately 3 μm. Samples for NMR experiments were prepared by filling standart 5 mm tubes with mixtures including 0, 40, 60, 80, and 100 wt. % 5CB; the height of the sample size was about 2 cm. The photopolymerization process was carried out under nitrogen atmosphere. The wavelength of the UV lamp (Hg-Xe) was fixed at $\lambda = 365$ nm using interferential filters. The UV irradiation intensity was 17.5 mW cm^{-2} and the irradiation time was set at 3 min [36]. In a recent study [35] the molecular weights and the polydispersities of PEHA films obtained from the same experimental conditions have been determined by gel permeation chromatography (GPC) yielding $M_w = 108\,000 \pm 5000$ g mol^{-1} and $M_w/M_n = 2.1 \pm 0.2$.

The polarized optical microscopy (POM) studies were performed on an Olympus BH2 microscope equipped with a heating/cooling stage Linkam TH-600 for the phase diagram determination, and on a Leica DMRXP microscope equipped with a heating/cooling stage Linkam LTS-350 for image processing. The phase diagram of the polymerized mixtures, noted PEHA/5CB, was obtained by using the following temperature treatment. In order to avoid any thermal history effects, samples were first heated from room temperature to a temperature located 15 °C above the isotropic phase limit, then quenched at 100 °C min^{-1} to 25 °C below the *N*-*I* transition. Samples were kept at this temperature for 30 min. Subsequently, another heating cycle with a rate of 1 °C min^{-1} up to the isotropic state was carried out. The whole procedure was repeated twice, and two independent samples of the same composition were analyzed. Final recording of the transition temperatures was made at the third heating ramp. The heating/cooling rates were chosen in a search for the most favorable conditions that allow reproducibility and clear identification of the transition temperature corresponding to morphology changes of the phase. These conditions were imposed by the requirement to reach the equilibrium of the system. For the heating ramp used, the transition temperatures were not modified, meaning that the system had reached equilibrium.

The ^{13}C-NMR experiments were performed at 100.58 MHz on a Varian UNITY/INOVA 400 NMR spectrometer ($\mathbf{B}_0 = 9.5T$) equipped with an indirect detection probe manufactured by Narolac Cryogenic Corporation, Martinez, CA. This probe maximizes the efficiency of proton decoupling and provides a temperature control of 0.1 °C. The temperature calibration was made by observing the nematic to isotropic transition of pure 5CB. The sample was spun at a slow rate (10 Hz) along the magnetic field $\mathbf{B}_0$. A recently developed broadband decoupling sequence, named SPINAL-64, exhibiting a high efficiency for removing all ^{1}H-^{13}C couplings, was used to yield sharp ^{13}C peaks [37]; ^{1}H-^{13}C cross polarization was not applied.

After the NMR experiment was finished, a small amount of each sample was taken from the NMR tube to perform DSC analysis and image processing; the sampling was carried out when the mixtures are homogeneous, i.e., in the isotropic state, to avoid changes in the LC/polymer ratio. The DSC measurements were performed on a Seiko DSC 220C calorimeter equipped with a liquid nitrogen system allowing cooling experiments. The DSC cell was purged with 50 ml min^{-1} of nitrogen. Rates of 10 °C min^{-1} (heating) and 30 °C min^{-1} (cooling) were used in the temperature range -100 °C to 100 °C. The method consists first in cooling the samples prior to heating and cooling cycles. The peaks of the clearing points were used to determine the nematic-isotropic transition temperature T_{NI} [38]. Typical DSC thermograms of linear polymer/LC systems have already been reported elsewhere [36,39] and are not presented here again. Droplet size measurements and image analysis were performed on a Macintosh PowerPC 7300/166 computer using the public domain NIH Image program [40].

III. RESULTS AND DISCUSSION

A. Phase diagram and morphology

Figure 2 shows the phase diagram of the polymerized mixture PEHA/5CB in the form of temperature versus LC weight fraction. The symbols represent POM and DSC data as indicated in the figure caption. One can see good agree-

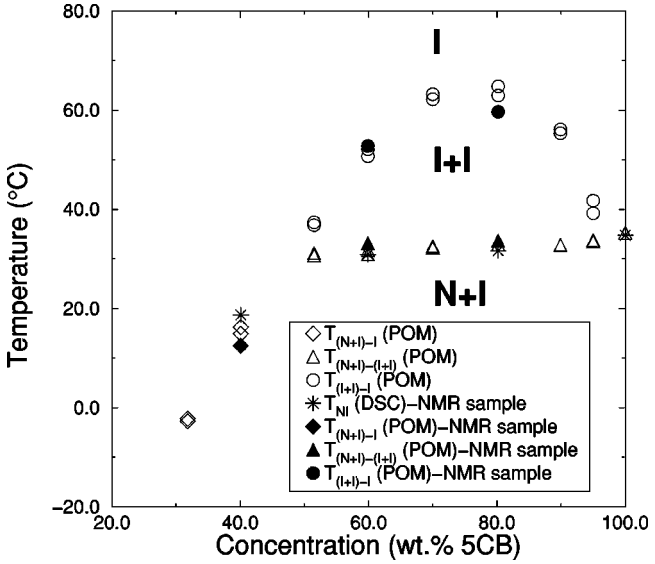

FIG. 2. Phase diagram of PEHA/5CB obtained from POM and DSC techniques. The open diamond, open triangle, and open circle symbols are averages of two series of samples from separate POM experiments. $T_{(N+I)-I}$, $T_{(N+I)-(I+I)}$ and T_{NI} represent the transition temperature of the phase separated liquid crystal between the nematic to isotropic states and $T_{(I+I)-(I)}$ is the isotropic+isotropic to isotropic transition temperature. The star and filled symbols are the data of samples taken from the NMR tubes after the NMR experiment was finished. The phase diagram exhibits three domains: nematic+isotropic $(N+I)$, isotropic+isotropic $(I+I)$, and isotropic (I).

ment between the two series of samples from separate POM experiments. The transition temperatures observed by POM for the NMR samples are consistent with the other POM data, indicating that the phase behavior is similar for samples prepared either between glass slides or in 5 mm NMR-tubes. DSC data obtained for the nematic to isotropic transition temperature T_{NI} are also in good agreement with the POM measurements. It is worth noting that the DSC thermograms did not show the $(I+I)$ to (I) transition [36,39]. The diagram exhibits an upper critical solution temperature (UCST) shape with three distinct regions. In the upper part of the phase diagram, the system exhibits a single isotropic (I) phase. When the temperature is lowered, a biphasic (isotropic+isotropic, $I+I$) region was observed. With further lowering of temperature, an isotropic polymer-rich phase is in equilibrium with a nematic LC phase (Fig. 3). In the range of LC compositions above 50 wt. % the $(N+I)$ to $(I+I)$ transition temperature is almost constant at about $T=33\,^{\circ}\mathrm{C}$, which corresponds approximately to the N-I transition temperature of bulk 5CB. This observation indicates that the phase-separated nematic LC domains are essentially pure. Between the triangle and circle symbols, the phase diagram exhibits a wide isotropic miscibility gap $(I+I)$ showing the high incompatibility between the polymer and the LC. It is interesting to note that the $(I+I)$ domain covers a range of temperature up to 30 °C near the critical point ($T_c \approx 63\,^{\circ}\mathrm{C}$, $\phi_c \approx 80$ wt. % 5CB) which is quite important compared to other linear polymer/LC blends [36,39,41]. For LC

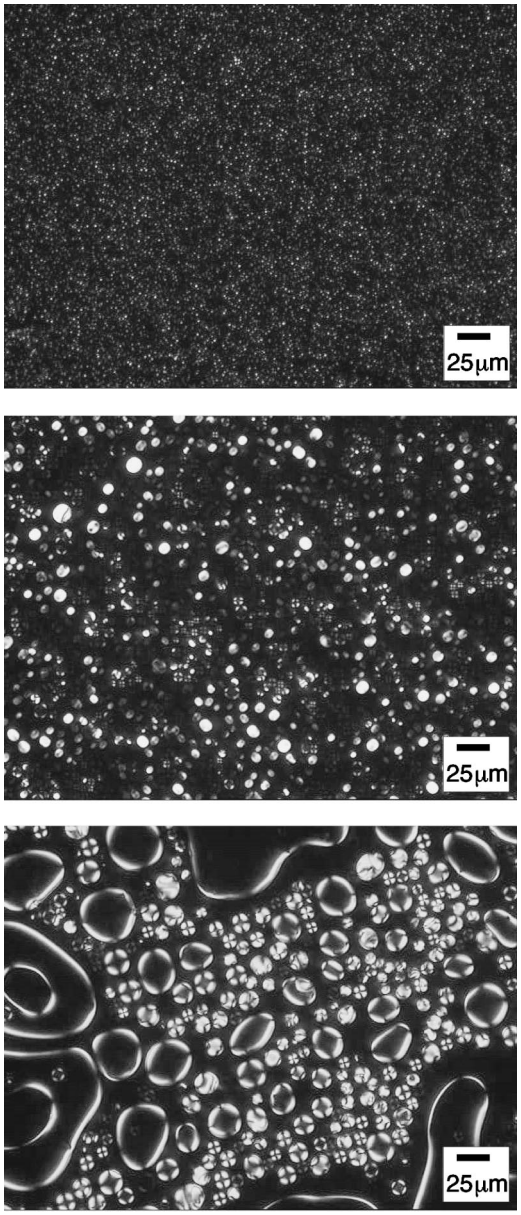

FIG. 3. Optical micrographs of PEHA/5CB samples taken at $T/T_{NI}=0.980$ (crossed polarizers mode, $P \perp A$, magnification $\times 200$) as a function of LC fraction: top, 40 wt. % 5CB; middle, 60 wt. % 5CB; bottom, 80 wt. % 5CB.

contents above 95 wt. %, no $(I+I)$ region was observed. This behavior has already been discussed in the literature [41,42] and is attributed to the difficulty to distinguish experimentally the transitions between the $(N+I)$ to (I) and the $(N+I)$ to $(I+I)$ regions. Dubault *et al.* [42] have shown that the phase separation process for polymer/LC mixtures with low polymer concentrations may require several days, which is beyond the time scale used for our experiments.

Samples in the isotropic state were taken from the NMR tubes after the NMR experiment was finished in order to compare the morphology of the systems under investigation. As for the phase diagram determination, samples were submitted to the same thermal treatment described in Sec. II. Due to the low viscosity of PEHA ($T_g \sim -62\,^{\circ}\mathrm{C}$) [35], coa-

lescence of neighboring droplets occurs at the early stages of the 30 min isotherm following the cooling ramp. After 10 min, the morphology of the sample does not change anymore, indicating that the system has reached equilibrium, or at least follows a very slow kinetic process. Figure 3 represents optical micrographs (crossed polarizers mode, $P \perp A$) of PEHA/5CB mixtures including from top to bottom 40, 60, and 80 wt. % of 5CB. Upon heating, optical micrographs were recorded at the same reduced temperature $T/T_{NI} = 0.980$ after 15 min under isothermal conditions; the textures of the samples remained unchanged, indicating that the thermodynamic equilibrium was reached. One can see that increasing the LC fraction leads to an increase in the size of the phase-separated LC domains. This behavior can be explained by the fact that the LC solubility limit in the polymer matrix is constant at a given temperature [35,36,39]. Therefore, increasing the LC content leads to an increase of the amount of phase separated LC. The increase in size of the nematic droplets might be related to a lower interfacial tension in the case of large droplets compared to smaller ones. The textures corresponding to samples prepared with 40 and 60 wt % of 5CB show nematic domains in the forms of droplets having a relatively narrow distribution with approximate mean diameters of 1 μm and 5 μm, respectively. For LC contents of 80 wt %, the morphology of the mixture exhibits important changes with mainly large nematic domains of several tens of microns and drops with an approximate mean diameter of 18 μm. For PEHA/5CB (40:60) and (20:80) systems, the nematic droplets exhibit a radial/axial structure [43–45], indicating that the director adopts a homeotropic anchoring at the polymer interface. This observation is in good agreement with previous works on alkyl brush surfaces and liquid crystal anchoring transitions at surfaces [15,35,48,49]. In the case of PEHA/5CB (60:40), the structure of the nematic droplets could not be determined optically even though a magnification of $\times 400$ was used; changes in the LC configuration are usually expected for droplets of radius ≈ 0.1 μm [5]. The influence of the cavity size on the orientational ordering of the phase-separated LC will be the subject the following section.

B. ^{13}C-NMR experiments

1. Theory

In a NMR experiment, the nematic liquid crystals have macroscopic alignment in the external magnetic field. With broadband proton decoupling, the ^{13}C-NMR spectra show resolvable peaks which can be assigned to individual carbon atoms. The chemical shifts of the observed signals (δ_{obs}) in the liquid crystalline phases are often considerably different from those in the isotropic state (δ_{iso}), and are determined by the order parameter tensor and the anisotropic chemical shift tensor:

$$\begin{aligned}\delta_{obs} &= \delta_{iso} + \delta_{aniso} \\ &= \delta_{iso} + \tfrac{1}{3} S_{zz}[\sigma_{zz} - \tfrac{1}{2}(\sigma_{zz} + \sigma_{yy})] \\ &\quad + \tfrac{1}{3}(S_{xx} - S_{yy})(\sigma_{xx} + \sigma_{yy}) + \tfrac{2}{3} S_{xy}\sigma_{xy} \\ &\quad + \tfrac{2}{3} S_{xz}\sigma_{xz} + \tfrac{2}{3} S_{yz}\sigma_{yz}, \end{aligned} \tag{3.1}$$

where the S_{ij} are components of the order parameter matrix, and the σ_{ij} are components of the chemical shift tensor in the axis system of the order parameter matrix.

For many cases, a semiempirical equation can be used to describe the relation between the observed chemical shift and the order parameter S_{zz} [33]:

$$\Delta\delta = \delta_{obs} - \delta_{iso} \approx \tfrac{2}{3} S_{zz} \Delta\sigma + b = a S_{zz} + b, \tag{3.2}$$

where $\Delta\sigma$ is the chemical shift anisotropy and is defined as

$$\Delta\sigma = [\sigma_{zz} - \tfrac{1}{2}(\sigma_{xx} + \sigma_{yy})]$$

and b is an empirical constant. The validity of Eq. (3.1) can be seen if one considers that the temperature dependence of the S_{zz} term is significant but the off-diagonal and biaxial terms are small so that their temperature dependence is negligible. For 1,4-disubstituted phenyl rings in liquid crystals, the C_2 axis is taken as the z axis. Then, the subscript zz is dropped and Eq. (3.1) can be rewritten to give

$$S = \alpha \Delta\delta + \beta, \tag{3.3}$$

where $\alpha = 1/a$ and $\beta = -b/a$. Because of the pretransitional effect [50], the values of δ_{iso} should be obtained at a temperature several degrees above the clearing point. It has been shown that the experimental results for several types of liquid crystals, including the cyanobiphenyl derivatives like 5CB, obey the semiempirical equations (3.2) and (3.3) very well [51–54].

To estimate the order parameter S of LC molecules confined in a polymer matrix, NMR experiments were carried out first on the pure compounds, i.e., PEHA and 5CB, then on (PEHA/5CB) mixtures having 40, 60, and 80 wt. % of 5CB, respectively.

2. ^{13}C-NMR *spectra*

Figure 4 displays typical NMR spectra of PEHA (a), isotropic 5CB (b), PEHA/5CB (40:60) at $T > T_{NI}$ (c), and PEHA/5CB (40:60) at $T < T_{NI}$ (d). Spectra for PEHA/5CB (60:40) and PEHA/5CB (20:80) are similar. The assignment of the spectra was done with the aid of the group contribution method [56]. All the NMR spectra exhibit well resolved peaks, even in the case of phase-separated LC domains in the nematic state [spectrum 4(d)]. The magnetic coherence length

$$\xi_B = \left(\frac{K\mu_0}{\Delta\chi \mathbf{B}_0^2} \right)^{1/2} \tag{3.4}$$

is of the order 800 nm [4,55]. However, ξ_B is based on the concept of strong anchoring, which may not be valid for the polymer matrix. In polymer/LC systems, anchoring forces can be relatively weak and the orientation at the surface competes with all other elastic deformations present in the droplet [10,57]. Therefore, ξ_B is probably smaller than 800 nm, and the high resolution spectra obtained allows us to assume that the director inside the droplets is aligned in the magnetic field $\mathbf{B}_0$ at $T < T_{NI}$ for the three PEHA/5CB mixtures under investigation.

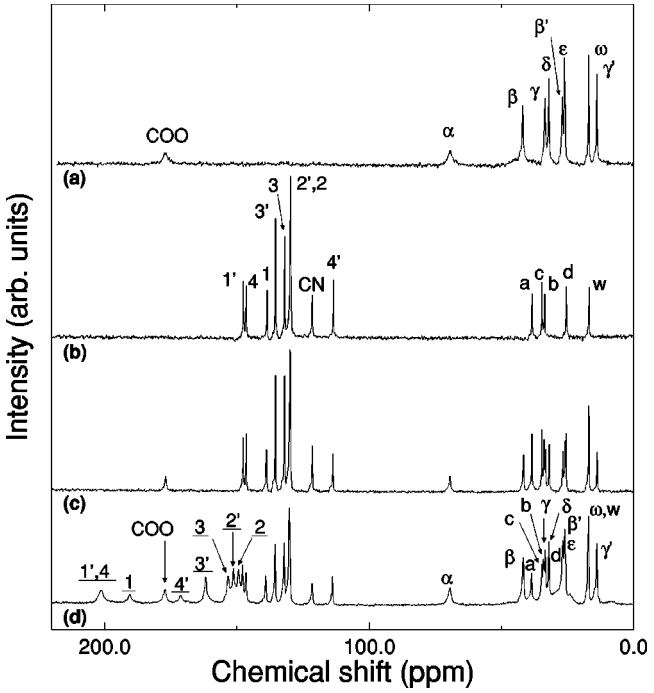

FIG. 4. Proton decoupled ^{13}C-NMR spectra at 100.58 MHz of PEHA (a), 5CB at $T>T_{NI}$ (b), PEHA/5CB (40:60) at $T>T_{NI}$ (c), and PEHA/5CB (40:60) at $T<T_{NI}$. The symbols refer to Fig. 1. The underlined numbers [spectrum (d)] correspond to the aromatic ^{13}C signals of the phase-separated 5CB in the nematic state ($T<T_{NI}$).

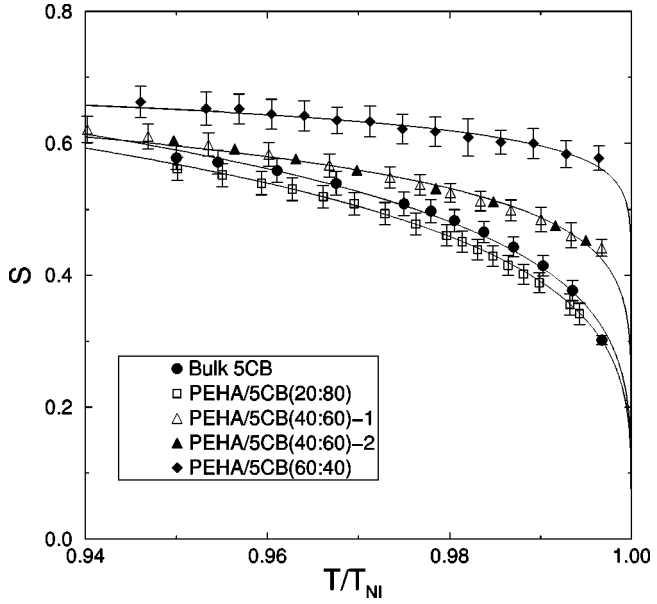

FIG. 5. Order parameter S of bulk 5CB and mixtures with 40, 60, and 80 wt. % of 5CB [calculated from Eq. (3.3) by the use of the parameters listed in Table II] plotted as a function of the reduced temperature T/T_{NI} from the ^{13}C chemical shift of the carbon atoms in the phenyl rings of 5CB molecules. The symbols represent averages of the experimental data of the eight aromatic carbons of the 5CB molecules and the solid lines are results of nonlinear least-squares fits of the experimental data to Eq. (3.5).

As expected, the NMR spectrum of PEHA [4(a)] does not show any aromatic carbon, and the peaks for the backbone carbons are very broad. In this region, only one peak is observed around 175 ppm corresponding to the carboxylate group COO. Spectrum 4(b) corresponds to 5CB in the isotropic state ($T>T_{NI}$). Both aromatic and aliphatic regions exhibit well resolved peaks. Spectrum 4(c) corresponds to the mixture PEHA/5CB (40:60) at $T>T_{NI}$. One can see that 4(c) is the sum of spectra 4(a) and 4(b). The isotropic ^{13}C signals of both pure compounds are observed. According to Eq. (3.1), the phase-separated anisotropic 5CB domains exhibit down-field-shifted aromatic signals at $T<T_{NI}$ [spectrum 4(d)], which are labeled with underlined symbols for clarity. In the aliphatic region, changes in the peak position are so small that signals for the two phases are not distinguishable (see Sec. III B 5). The aromatic NMR signals were used for the order parameter calculation due to a higher chemical shift anisotropy [31]. It is interesting to note that isotropic 5CB signals are still observed, which correspond to the amount of 5CB molecules dissolved in the polymer matrix [39,35,36] (see Sec. III B 4).

3. Order Parameter of bulk and confined 5CB

To estimate the order parameter S using Eq. (3.3), the chemical shift anisotropy $\Delta\delta$ of each aromatic carbon is measured from NMR spectra recorded at several given temperatures. Then calculated values of α (ppm^{-1}) and β (unitless) were used (Table I) to determine S. Figure 5 displays the evolution of the order parameter S versus the reduced temperature T/T_{NI} for bulk 5CB and mixtures with 40, 60, and 80 wt % of 5CB. In order to check the reproducibility of the measurements, two independent experiments were carried out on the same PEHA/5CB (40:60) sample with one month delay. Both open ($t=0$) and filled ($t=1$ month) triangles show the same behavior. These results also confirm that the samples had reached equilibrium with the temperature treatment used. In Fig. 5 the symbols represent averages of experimental data of the eight aromatic carbons of the 5CB molecules, and the solid lines are the best fit curves using the Haller equation [58]

TABLE I. Calculated values of α (ppm^{-1}) and β (unitless) for each ^{13}C nucleus in the phenyl rings (see Fig. 1) in alkyl cyanobiphenyl derivatives nCB [51].

	Carbon nucleus							
	1	2	3	4	1′	2′	3′	4′
α	0.0124	0.0339	0.0315	0.0117	0.0122	0.0326	0.0238	0.0108
β	−0.08	−0.10	−0.12	−0.09	−0.09	−0.16	−0.10	−0.07

$$S(T)=S_0\left(1-\frac{T}{T_{NI}}\right)^F, \tag{3.5}$$

where S_0 and F are empirical parameters. The orientational ordering of bulk 5CB was found to be similar to those reported in the literature [33,51] and was used as a reference for comparison with the three other systems. The sample prepared with 20 wt. % of PEHA [PEHA/5CB(20:80)] behaves like bulk 5CB, but the values lies slightly below the curve of pure LC. This behavior can be explained by the morphology of the sample; large nematic domains are separated by an isotropic phase rich in the polymer PEHA, which can alter the alignment of the director in the magnetic field $\mathbf{B}_0$ leading to a slight decrease of the macroscopic order parameter. In the case of mixtures including 40 and 60 wt. % of PEHA [PEHA/5CB(40:60), PEHA/5CB(60:40)], the 5CB molecules are confined in droplets of 5 and 1 μm, respectively. One can clearly see that the nematic order parameter S increases with decreasing droplet size, and is always higher than bulk 5CB. It is interesting to note that previous NMR works on relaxation studies of polymer/5CB systems have shown that the relaxation rates (e.g., $T_{1\rho}^{-1}, T_2^{-1}$) increase with decreasing droplet size [24,26]. The increase in polymer/LC contact in the smaller droplets significantly limits the mobility of the LC in the droplets compared to that of the LC in larger volume domains. The optical observations indicate that PEHA induces a homeotropic anchoring of the nematic director in the droplets. Therefore, the polymer surface influences the surface orientational order and may lead to an increase of the nematic order in smaller cavities. This explanation may not be fully satisfying because the spherical shape of the droplets would tend to reduce the orientational order due to the surface effect which would favor a more spherical distribution of the director. The first alternative explanation might be associated with the change in the volume of the director configuration in small droplets. Indeed, as for different size nematic droplets in the presence of an applied electric field [45,46], the magnetic field might induce director configuration transformation (e.g., radial↔axial), and lead to an increase of the order parameter of the confined LC in smaller droplets. The second alternative explanation might be associated with the presence of a small amount [47] of oligomeric or polymeric PEHA chains dissolved in the nematic phase. These chains could also influence the orientational order in the way which is observed.

The values obtained from the least squares fit of the experimental data to Eq. (3.5) are listed in Table II. It should be pointed out that Eq. (3.5) is an empirical relation which may be regarded as a special case of the Landau–de Gennes theory in describing the molecular ordering for isotropic-nematic transitions [50], but it is not strictly valid near the clearing temperature [58]. The physical meaning of the parameters S_0 and F is quite simple: S_0 is the limit of the order parameter with decreasing temperature, and F may be considered as an indication of how quickly a molecular segment reaches the limit of the order parameter as a function of change in temperature. Experimentally, the limiting value of the order parameter S_0 cannot be reached due to phase transition of the liquid crystal into a solid. The S_0 values of 5CB and PEHA/5CB (20:80) are found to be larger than one, which is physically impossible. For pure LC compounds [33,51], the accuracy of these values is comparable to that of the order parameter (i.e., 5–10 %). It should be pointed out that the errors indicate the quality of the fitting, not necessarily the errors of the model. As previously discussed, the order parameters of 5CB and PEHA/5CB(20:80) samples behave in the same way, leading to similar S_0 and F values. For blends including 60 and 40 wt. % of 5CB, one can clearly see the influence of the confinement on the parameter F. Indeed, F decreases with decreasing droplet size indicating that the molecular segment reaches the limit of the order parameter more slowly in smaller cavities than in the case of larger nematic domains.

TABLE II. Parameters for the temperature dependence of S for the phenyl rings obtained from fitting the data to Eq. (3.5). R is the correlation factor. The accuracy of S_0 and F is comparable to that of the order parameter, i.e., 5–10 %.

	S_0	F	R
5CB	1.147	0.222	0.982
PEHA/5CB(20:80)	1.142	0.233	0.981
PEHA/5CB(40:60)	0.867	0.125	0.985
PEHA/5CB(60:40)	0.768	0.055	0.987

4. Nematic fraction of phase-separated 5CB

As discussed in Sec. III A, the transition temperatures observed by POM for the NMR samples are consistent with POM data obtained for samples prepared between glass slides. The phase diagram presented gives the evolution of the observed nematic-isotropic transition temperature as a function of the *initial* LC content in the polymer/LC mixture. Due to the polymerization-induced phase separation process, LC molecules remain dissolved in the isotropic polymer rich phase, meaning that the phase diagram cannot be used to determine the fraction of phase-separated LC. In order to estimate compositions and amounts of the coexisting phases, other experimental techniques such as DSC or image processing need to be used. In this section we demonstrate that NMR data can also be used to determine these quantities. By integrating a given aromatic LC peak of spectrum 4(d) in both isotropic and anisotropic regions (Fig. 4), the nematic fraction of 5CB F_N contained in the LC droplets can be estimated by calculating the ratio

$$F_N=\frac{I^N}{I^N+I^I}, \tag{3.6}$$

where I^N is the peak intensity in the nematic phase, and I^I is the peak intensity in the isotropic state. Figure 6 shows the calculated nematic fraction using the signals of 3′ and 1 carbon atoms of the three mixtures as a function of the reduced temperature T/T_{NI}. The 3′ and 1 aromatic peaks were chosen because they are well resolved in both isotropic and anisotropic regions. The evolution of the nematic fraction as

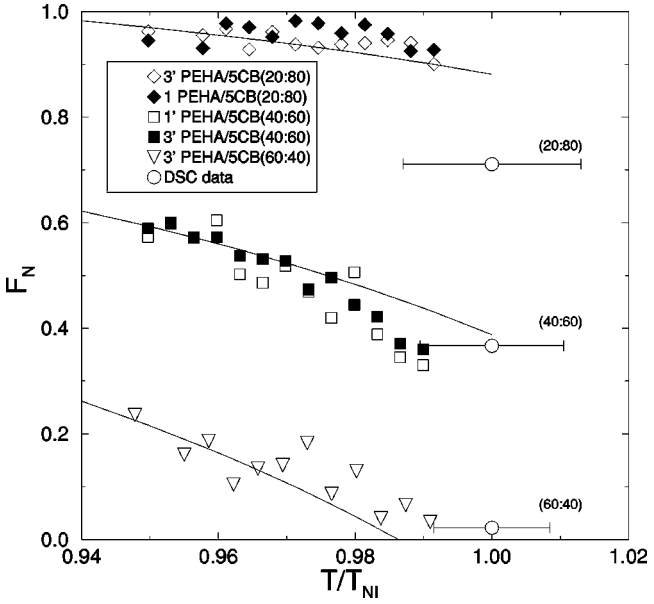

FIG. 6. Nematic fraction of 5CB F_N in samples including 40, 60, and 80 wt. % of liquid crystals as a function of the reduced temperature T/T_{NI}. The diamond, square, and triangle symbols represent the nematic fraction deduced from the NMR spectra, whereas the open circles represent the nematic fraction calculated from DSC measurements using Eq. (3.12); the horizontal bars correspond to the temperature range of measurement of ΔH_{NI}. The solid lines represent nonlinear least-squares fitting of the NMR results to Eq. (3.11), with $a=0.21$, $a'=-2.70$, $b=3.15$, $b'=5.65$, and $y=0.8$, 0.6, and 0.4, respectively (correlation factor $R=0.981$).

a function of temperature can be determined by using the following model: in phase I (LC-rich phase), the fraction of nematic 5CB (component *A*) is f^N and the fraction of PEHA (component *B*) is $(1-f^N)$; in phase II (polymer-rich phase), the fraction of isotropic 5CB (dissolved in the polymer matrix) is f^I and the fraction of PEHA is $(1-f^I)$.

If the systems are at equilibrium, f^N and f^I remain constant with total composition, i.e., the fraction of 5CB is y (40, 60, and 80 wt. %, respectively). For the two phases, phase I has a nematic fraction F_N, and phase II has $(1-F_N)$. This leads to

$$[f^N A+(1-f^N)B]F_N+[f^I A+(1-f^I)B](1-F_N) = yA+(1-y)B. \tag{3.7}$$

By rearranging, then by equating the coefficients *A* and *B*, the nematic fraction F_N can be expressed as

$$F_N=\frac{y-f^I}{f^N-f^I}. \tag{3.8}$$

According to Drzaic [10], the liquid crystal solubility in PDLC samples evolves linearly versus the temperature, meaning that the dependence of f^N and f^I on temperature $[T/T_{NI}(x)]$ can be described by linear functions

$$f^N=a+bx, \tag{3.9}$$

$$f^I=a'+b'x. \tag{3.10}$$

Therefore,

$$F_N=\frac{x-a'-b'x}{(a-a')+(b'-b)x}, \tag{3.11}$$

where the parameters a, a', b, b', can be obtained from nonlinear least-squares fitting of *all* the experimental data with a defined parameter y for each LC content and one independent variable x. In Fig. 6, the solid lines represent the fit curves of the nematic fraction values calculated from the NMR data to Eq. (3.11). One can see that there is a reasonable agreement between the simple theoretical model describing F_N and the experimental NMR results.

The relative amount γ of LC contained in the nematic droplets can also be deduced from the thermodynamic quantities accessible from the DSC data. The nematic-isotropic transition enthalpy ΔH_{NI} can be used to calculate γ [35,36,59,60],

$$\gamma=\frac{m_{LC}^D}{m_{LC}}=\left(1+\frac{m_P}{m_{LC}}\right)P(x)=\left(\frac{100}{x}\right)P(x), \tag{3.12}$$

where m_{LC}^D represents the mass of LC included in the droplets, while m_P and m_{LC} are the masses of the polymer and the LC in the sample, respectively. $P(x)$ represents the ratio between the nematic-isotropic transition enthalpy for a LC polymer composite material and the equivalent value for the pure LC

$$P(x)=\frac{\Delta H_{NI}(x)}{\Delta H_{NI}(LC)}. \tag{3.13}$$

In Fig. 6 the nematic LC fractions γ determined by applying Eq. (3.12) are represented by open circles and the horizontal bars correspond to the temperature range of measurement of ΔH_{NI} (i.e., the *N-I* transition DSC peak width). One can clearly see that the nematic fraction at room temperature is underestimated if Eq. (3.12) is used. Even though the DSC technique is a convenient method, the nematic fraction is only determined around the *N-I* transition whereas the NMR experiments give the evolution of the nematic fraction over the whole temperature range of interest.

5. Polymer/LC interface

In Sec. III A the optical observations have shown that PEHA induces a homeotropic alignment at the polymer/LC interface. The pendant aliphatic chains of PEHA (i.e., the 2-ethylhexyl fragment) are known to provoke a surface-induced order [15,35,48,49]. NMR investigations have been carried out in the aliphatic region in order to get further informations on the orientational ordering of the polymer chains. The chemical shifts $\Delta\delta$ of four well resolved aliphatic peaks belonging to the 2-ethylhexyl fragment (ω, δ, δ', γ) were studied as a function of temperature. In Fig. 7 the case of the PEHA/5CB (40:60) system is presented, and a similar behavior was observed for the two other mixtures, including 40 and 80 wt. % 5 CB. The evolution of $\Delta\delta$ vs T/T_{NI} exhibits

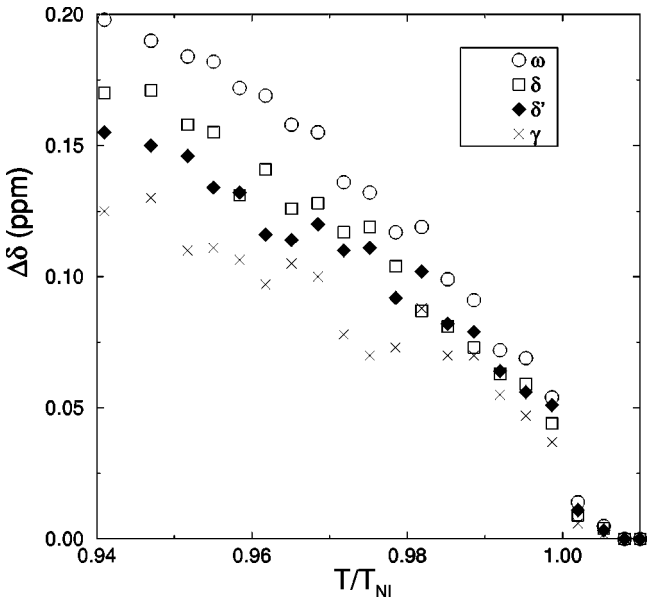

FIG. 7. Evolution of the anisotropic chemical shifts $\Delta\delta$ of the PEHA aliphatic carbons ω, δ, δ', and γ as a function of the reduced temperature T/T_{NI}.

the same trend as that of the nematic order parameter *S*, i.e., a nonlinear decrease when $T/T_{NI}\rightarrow 1$, characteristic of a first order phase transition. The presence of these small but distinct chemical shifts changes is caused by an induced orientational ordering of the PEHA molecules in direct contact with 5CB. These molecules are in the *N* phase, and are probably in rapid exchange with those dissolved in the isotropic polymer-rich phase, so that the observed peaks are weighted average signals. It is also interesting to note that the farther the pendant aliphatic carbon of PEHA, the higher is the chemical shift anisotropy, indicating a higher order parameter for the corresponding C-H bond. This may be the result of interdigitation between the 2-ethylhexyl fragments and the 5CB molecules, which makes the carbon atoms located at the end of the hexyl chain have closer interaction with the LC molecules and therefore be more strongly influenced by the nematic order. Immediately above the phase transition, $\Delta\delta$ is not zero, indicating that a weak pretransitional effect occurs. This behavior is of the same order of magnitude as that of 5CB. Indeed above $T/T_{NI}=0.98$, the NMR signals of carbon atoms ω (polymer) and *w* (5CB) overlap (see Fig. 4). The pretransitional behavior shown by the polymer may be the result of interdigitation between the 2-ethylhexyl fragments and the nematogen and imprinting order of the lateral aliphatic chains of PEHA.

IV. CONCLUSIONS

The morphology and the phase behavior of PEHA/5CB blends were studied by polarized optical microscopy, ^{13}C-NMR spectroscopy, and DSC. The experimental phase diagram obtained exhibits a typical UCST shape. The existence of a $(I+I)$ miscibility gap between the $(N+I)$ domain and a single isotropic phase has been clearly shown. The order parameter determination method initially developed by Guo and Fung [33] for bulk LC has been successfully applied to these PDLC samples. This technique has the major advantage of not requiring the use of deuterated LC to study the order parameter. The nematic order parameter *S* increases with decreasing droplet size which may result from increased polymer/LC surface contacts in smaller cavities. From the NMR data, the nematic fraction has been determined over the whole temperature range of interest and compared to the fractional amount of LC contained in the droplets deduced from DSC measurements. It has been found that the nematic fraction is underestimated when the DSC method is used. NMR investigations in the aliphatic region of the spectra have shown that the 2-ethylhexyl fragment of the polymer chain is partially ordered at the polymer/LC interface due to interdigitation with 5CB molecules. Above the *N*-*I* transition, a weak pretransitional effect has been observed resulting from interdigitation of PEHA fragments with the nematogen and imprinting order of the lateral aliphatic polymer chains. This useful NMR method opens the field of further studies involving PDLC samples prepared with various macromolecular architectures and different surface anchoring conditions. PDLC systems developed for electrooptical applications might also be investigated by this method in order to study the influence of the order parameter of confined LC on the electro-optical properties.

ACKNOWLEDGMENTS

This work was performed during a stay of F.R. at the University of Oklahoma. Professor J. M. Buisine is acknowledged for his contribution. This research was funded in part by the MENRT, the Région Nord-Pas de Calais, the FEDER, and the CNRS. The work of B.M.F. was supported by the Air Force Office of Scientific Research (Grant No. F9620-98-1-0453) and the Oklahoma State of Regents for Higher Education (Grant No. CHK000021).

[1] G. P. Crawford and S. Žumer, *Liquid Crystals in Complex Geometries* (Taylor and Francis, London, 1996).
[2] S. Stapf, R. Kimmich, and R. Seitter, Phys. Rev. Lett. **75**, 2855 (1995).
[3] G. Schwalb and F. W. Deeg, Phys. Rev. Lett. **74**, 1383 (1995).
[4] C. Cramer, T. Cramer, F. Kremer, and R. Stannarius, J. Chem. Phys. **106**, 3730 (1997).
[5] A. Golemme, S. Žumer, D. W. Allender, and J. W. Doane, Phys. Rev. Lett. **61**, 2937 (1988).
[6] P. Sheng, Phys. Rev. Lett. **37**, 1059 (1976).
[7] P. Sheng, Phys. Rev. A **26**, 1610 (1982).
[8] G. P. Crawford, R. Stannarius, and J. W. Doane, Phys. Rev. A **44**, 2558 (1991).
[9] G. P. Crawford, D. W. Allender, and J. W. Doane, Phys. Rev. A **45**, 8693 (1992).
[10] P. S. Drzaic, *Liquid Crystals Dispersions* (World Scientific, Singapore, 1995).
[11] G. S. Iannachione, G. P. Crawford, S. Žumer, J. W. Doane, and

D. Finotello, Phys. Rev. Lett. **71**, 2595 (1993).
[12] T. Bellini, N. A. Clark, and D. W. Schaefer, Phys. Rev. Lett. **74**, 2740 (1995).
[13] S. A. Carter *et al.*, J. Appl. Phys. **81**, 5992 (1997); **55**, 1646 (1997).
[14] K. Amundson, A. van Blaaderen, and P. Wiltzius, Phys. Rev. E **55**, 1646 (1997).
[15] K. R. Amundson and M. Srinivasarao, Phys. Rev. E **58**, R1211 (1998); K. R. Amundson, *ibid.* **58**, 3273 (1998).
[16] G. P. Crawford *et al.*, Liq. Cryst. **14**, 1573 (1993).
[17] C. A. McFarland, J. L. Koenig, and J. L. West, Appl. Spectrosc. **47**, 598 (1993).
[18] C. L. Khetrapal, K. V. Ramanathan, and G. A. Nagana Gowda, in *Nuclear Magnetic Resonance* (The Royal Society of Chemistry, London, 2000), Vol. 29, p. 534.
[19] F. M. Aliev, in *Liquid Crystals in Complex Geometries*, edited by G. P. Crawford and S. Žumer (Taylor and Francis, London, 1996), p. 345.
[20] Y. K. Fung *et al.*, Phys. Rev. E **55**, 1637 (1997).
[21] D. Finotello, G. S. Innachione, and S. Qian, in *Liquid Crystals in Complex Geometries* (Ref. [19]), p. 325.
[22] C. W. Cross and B. M. Fung, J. Chem. Phys. **96**, 7086 (1992); **99**, 1425 (1993); B. M. Fung and C. W. Cross, Magn. Reson. Imaging **9**, 717 (1991).
[23] M. Ambrožvzič, P. Formoso, A. Golemme, and S. Žumer, Phys. Rev. E **56**, 1825 (1997).
[24] M. Vilfan *et al.*, J. Chem. Phys. **103**, 8726 (1995); M. Vilfan *et al.*, Phys. Rev. E **59**, R4754 (1999).
[25] P. A. Mirau and M. Srinivasarao, Appl. Spectrosc. **51**, 1639 (1997).
[26] K. L. Buchert, J. L. Koenig, S.-Q. Wang, and J. L. West, Appl. Spectrosc. **47**, 933 (1993); **47**, 942 (1993).
[27] D. Schwartz-Haller, F. Noack, M. Vilfan, and G. P. Crawford, J. Chem. Phys. **105**, 4823 (1996).
[28] A. Riede, S. Grande, A. Hohmuth, and W. Weissflog, Liq. Cryst. **22**, 157 (1997).
[29] C. Chiccoli, P. Pasini, G. Skačej, C. Zannoni, and S. Žumer, Phys. Rev. E **60**, 4219 (1999).
[30] C. Chiccoli, P. Pasini, G. Skačej, C. Zannoni, and S. Žumer, Phys. Rev. E **62**, 3766 (2000).
[31] B. M. Fung, in *Encyclopedia of Nuclear Magnetic Resonance*, edited by D. M. Grant and R. K. Harris (Wiley Publishers, Chichester, England, 1996), p. 2744.
[32] J. W. Emsley, *Nuclear Magnetic Resonance of Liquid Crystals* (Reidel, Dordrecht, 1985).
[33] W. Guo and B. M. Fung, J. Chem. Phys. **95**, 3917 (1991); **97**, 8819 (1992).
[34] Value given by Merck Ltd., Merck House, Poole, Great Britain.
[35] F. Roussel *et al.*, Phys. Rev. E **62**, 2310 (2000).
[36] F. Roussel, J.-M. Buisine, U. Maschke, and X. Coqueret, Liq. Cryst. **24**, 555 (1998); F. Roussel, Ph.D. thesis, Université du Littoral–Côte d'Opale, France, 1996.
[37] B. M. Fung, K. Ermolaev, and A. K. Khitrin, J. Magn. Reson. **142**, 97 (2000).
[38] The *N-I* transitions observed for the PEHA/5CB systems are quite broad leading to great uncertainties in the determination of the temperature onset.
[39] F. Benmouna *et al.*, J. Polym. Sci., Polym. Phys. Ed. **37**, 1841 (1999); Macromolecules **33**, 960 (2000).
[40] NIH image was developed at the U.S. National Institutes of Health and is available on the Internet at http://rsb.info.nih.gov/nih-image/.
[41] W. Ahn, C. Y. Kim, H. Kim, and S. C. Kim, Macromolecules **25**, 5002 (1992).
[42] A. Dubault, C. Casagrande, and M. Veyssie, Mol. Cryst. Liq. Cryst. Lett. **72**, 189 (1982).
[43] H. S. Kitzerow, Liq. Cryst. **16**, 1 (1994).
[44] R. Ondris-Crawford *et al.*, J. Appl. Phys. **69**, 6380 (1991).
[45] G. P. Crawford and J. W. Doane, Condens. Matter News **1**, 5 (1992).
[46] J. H. Erdmann, S. Žumer, and J. W. Doane, Phys. Rev. Lett. **64**, 1907 (1990).
[47] This amount is probably very small because the nematic-isotropic transition temperature remains nearly constant for LC content ranging from 50 to 95 wt. %, indicating that the phase separated LC is essentially pure.
[48] J. E. Proust, L. Ter-Minassian-Saraga, and E. Guyon, Solid State Commun. **11**, 1127 (1972).
[49] G. P. Crawford, R. J. Ondris-Crawford, J. W. Doane, and S. Žumer, Phys. Rev. E **53**, 3647 (1996).
[50] M. L. Magnuson, B. M. Fung, and J.-P. Bayle, Liq. Cryst. **19**, 823 (1995).
[51] T.-H. Tong, B. M. Fung, and J. P. Bayle, Liq. Cryst. **22**, 165 (1997).
[52] F. Roussel *et al.*, Liq. Cryst. **26**, 251 (1999).
[53] J.-P. Bayle and B. M. Fung, Liq. Cryst. **15**, 87 (1993).
[54] M. L. Magnuson, B. M. Fung, and M. Schadt, Liq. Cryst. **19**, 333 (1995).
[55] M. Vilfan and N. Vrbančič-Kopač, in *Liquid Crystals in Complex Geometries* (Ref. [19]), p. 159.
[56] H. O. Kalinowski, S. Berger, and S. Braun, *Carbon-13 NMR Spectroscopy* (Wiley and Sons, Chichester, England, 1988).
[57] B. Jérôme, *Handbook of Liquid Crystals*, edited by D. Demus, J. Goodby, G. W. Gray, H.-W. Spiess, and V. Vill (Wiley-VCH, Weinheim, 1998).
[58] I. Haller, Prog. Solid State Chem. **10**, 103 (1975).
[59] G. W. Smith and N. A. Vaz, Liq. Cryst. **3**, 543 (1988); G. W. Smith, Mol. Cryst. Liq. Cryst. **180B**, 201 (1990).
[60] F. Roussel, U. Maschke, J.-M. Buisine, and X. Coqueret, C. R. Acad. Sci., Ser. IIb: Mec., Phys., Chim., Astron. **326**, 449 (1998).